

Transverse Double-Spin Asymmetries for Muon Pair Production in pp Collisions

O. Martin, A. Schäfer

Institut für Theoretische Physik, Universität Regensburg, D-93040 Regensburg, Germany

M. Stratmann

Department of Physics, University of Durham, Durham, DH1 3LE, England

W. Vogelsang

*Theory Division, CERN, CH-1211 Geneva 23, Switzerland; now at:
Institute for Theoretical Physics, State Univ. of New York at Stony Brook, NY-11794, USA*

(June 24, 1999)

We calculate the rapidity dependence of the transverse double-spin asymmetry for the Drell-Yan process to next-to-leading order in the strong coupling. Input transversity distributions are obtained by saturating the Soffer inequality at a low hadronic mass scale. Results for the polarized BNL-RHIC proton-proton collider and the proposed HERA- \vec{N} fixed-target experiment are presented, and the influence of the limited muon acceptance of the detectors on measurements of the asymmetry is studied in detail.

One of the major goals of the forthcoming spin programme at the RHIC polarized proton-proton collider [1] is a first measurement of the twist-2 transversity distribution $\delta q(x, \mu^2)$ [2], which is theoretically as important as the well-known unpolarized and longitudinally polarized parton densities $q(x, \mu^2)$ and $\Delta q(x, \mu^2)$, respectively. An important, non-trivial model-independent restriction on the size of $\delta q(x, \mu^2)$ derives from Soffer's inequality [3], which states that

$$|\delta q(x, \mu^2)| \leq \frac{1}{2} [q(x, \mu^2) + \Delta q(x, \mu^2)] , \quad (1)$$

and similarly for antiquarks. It was shown to be preserved by next-to-leading order (NLO) DGLAP evolution in "reasonable" factorization schemes, among them the $\overline{\text{MS}}$ -scheme [4-6].

In a previous NLO analysis, see [5] for details, we have derived an upper bound [by saturating (1)] for the total transverse double-spin asymmetry $A_{TT}(M)$ for Drell-Yan dimuon production of mass M . It turned out, however, that $A_{TT}(M)$ is not very sensitive to the *shape* of δq . In addition the angular acceptance of the detectors was assumed to be constant, i.e., independent of the dimuon rapidity y , which can only be a rather crude approximation to the real experimental conditions. Therefore, in order to better suit the experimental needs, we extend the analysis of [5] in this note and study the y dependence of A_{TT} .

The transversely polarized Drell-Yan cross section, $d\delta\sigma \equiv (d\sigma^{\uparrow\uparrow} - d\sigma^{\uparrow\downarrow})/2$, is given as a double convolution of transversity distributions with the corresponding transversely polarized partonic cross section:

$$\frac{d\delta\sigma}{dMdyd\phi} = \sum_q \tilde{e}_q^2 \int_{x_1^0}^1 dx_1 \int_{x_2^0}^1 dx_2 [\delta q(x_1, \mu_F^2) \delta \bar{q}(x_2, \mu_F^2) + \delta \bar{q}(x_1, \mu_F^2) \delta q(x_2, \mu_F^2)] \frac{d\delta\hat{\sigma}}{dMdyd\phi} , \quad (2)$$

μ_F being the factorization scale. The effective charge \tilde{e}_q also contains the electroweak effects from Z^0 exchange and γZ^0 interference; see, e.g., Eq. (20) of [5]. y denotes the rapidity of the dimuon pair, and ϕ is the azimuthal angle of one muon, with $\phi = 0$ in the direction of positive transverse spin of the incoming protons. The variables x_1^0, x_2^0 in (2) are related to y and the Drell-Yan scaling variable $\tau = M^2/S$ by $x_1^0 = \sqrt{\tau}e^y$ and $x_2^0 = \sqrt{\tau}e^{-y}$, so that the region $y > 0$ ($y < 0$) is mainly sensitive to x_1^0 (x_2^0). To lowest order (LO) x_1^0 and x_2^0 coincide with the momentum fractions carried by the incident partons. Indeed, one has at LO¹:

$$\frac{d\delta\hat{\sigma}^{(0)}}{dMdyd\phi} = \frac{2\alpha^2}{9SM} \cos(2\phi) \delta(x_1 - x_1^0) \delta(x_2 - x_2^0) . \quad (3)$$

In the $\overline{\text{MS}}$ -scheme, the NLO [$\mathcal{O}(\alpha_s)$] correction to (3) reads

¹The formula $\Phi(\phi) = 1$ below Eq. (15) in [5] should read $\Phi(\phi) = 2$.

$$\begin{aligned}
\frac{d\delta\hat{\sigma}^{(1),\overline{\text{MS}}}}{dMdyd\phi} &= \frac{2\alpha^2}{9SM} C_F \frac{\alpha_s(\mu_R^2)}{2\pi} \frac{4\tau(x_1x_2 + \tau)}{x_1x_2(x_1 + x_1^0)(x_2 + x_2^0)} \cos(2\phi) \\
&\times \left\{ \delta(x_1 - x_1^0)\delta(x_2 - x_2^0) \left[\frac{1}{4} \ln^2 \frac{(1 - x_1^0)(1 - x_2^0)}{\tau} + \frac{\pi^2}{4} - 2 \right] \right. \\
&+ \delta(x_1 - x_1^0) \left[\frac{1}{(x_2 - x_2^0)_+} \ln \frac{2x_2(1 - x_1^0)}{\tau(x_2 + x_2^0)} + \left(\frac{\ln(x_2 - x_2^0)}{x_2 - x_2^0} \right)_+ + \frac{1}{x_2 - x_2^0} \ln \frac{x_2^0}{x_2} \right] \\
&+ \frac{1}{2[(x_1 - x_1^0)(x_2 - x_2^0)]_+} + \frac{(x_1 + x_1^0)(x_2 + x_2^0)}{(x_1x_2^0 + x_2x_1^0)^2} - \frac{3 \ln \left(\frac{x_1x_2 + \tau}{x_1x_2^0 + x_2x_1^0} \right)}{(x_1 - x_1^0)(x_2 - x_2^0)} \\
&\left. + \ln \frac{M^2}{\mu_F^2} \left[\delta(x_1 - x_1^0)\delta(x_2 - x_2^0) \left(\frac{3}{4} + \frac{1}{2} \ln \frac{(1 - x_1^0)(1 - x_2^0)}{\tau} \right) + \delta(x_1 - x_1^0) \frac{1}{(x_2 - x_2^0)_+} \right] \right\} + [1 \leftrightarrow 2], \quad (4)
\end{aligned}$$

where μ_R is the renormalization scale (for simplicity we always take $\mu_R \equiv \mu_F = M$) and ($i = 1, 2$)

$$\int_{x_i^0}^1 dx_i f(x_i) \frac{1}{(x_i - x_i^0)_+} \equiv \int_{x_i^0}^1 dx_i \frac{f(x_i) - f(x_i^0)}{x_i - x_i^0}. \quad (5)$$

Equation (4) is obtained by a suitable factorization-scheme transformation of the corresponding result of [7], which was calculated taking the gluon off-shell in the process $q\bar{q} \rightarrow \mu^+\mu^-g$ in order to regularize its collinear divergences. The corresponding results for the unpolarized NLO cross section $d\sigma \equiv (d\sigma^{\uparrow\uparrow} + d\sigma^{\uparrow\downarrow})/2$ can be found in [8]².

In order to increase the observable rates, we will integrate the unpolarized cross section over ϕ , whereas in the polarized case we add each quadrant with a different sign. Thus, the rapidity dependent asymmetry will be defined as

$$A_{TT}(y) \equiv \frac{\int_{M_0}^{M_1} dM \left(\int_{-\pi/4}^{\pi/4} - \int_{\pi/4}^{3\pi/4} + \int_{3\pi/4}^{5\pi/4} - \int_{5\pi/4}^{7\pi/4} \right) d\phi \, d\delta\sigma/dMdyd\phi}{\int_{M_0}^{M_1} dM \int_0^{2\pi} d\phi \, d\sigma/dMdyd\phi}, \quad (6)$$

where $M_{0,1}$ denote the limits of some suitable bin in invariant mass. Following closely our previous study [5] on the total (i.e. y -integrated) Drell-Yan cross section, we will try to estimate *upper bounds* on A_{TT} by assuming that the *equality* in (1) holds³ at a low hadronic mass scale $\mu_0 \simeq \mathcal{O}(0.6 \text{ GeV})$, see [5] for more details. We should emphasize that the *sign* of the asymmetry cannot be predicted in this way, because only the absolute value of δq enters Soffer's inequality. This also means that all possible combinations of signs in Eq. (1) must be checked so as to obtain the maximal absolute value of A_{TT} . In our case, choosing all signs to be the same always yielded the largest results.

Figures 1 and 2 show the “maximally possible” $d\delta\sigma/dy$ and A_{TT} in LO and NLO for $\sqrt{S} = 500 \text{ GeV}$ at RHIC and for $E_{\text{beam}} = 820 \text{ GeV}$, corresponding to $\sqrt{S} = 39.2 \text{ GeV}$, at HERA- \vec{N} , respectively. We have integrated over M in (6) as indicated in the figures, avoiding masses smaller than 5 (4) GeV for RHIC (HERA- \vec{N}), where a large background from charmed-meson decay is expected. Very similar results as in Fig. 1 are obtained for $\sqrt{S} = 200 \text{ GeV}$ and $\mathcal{L} = 320 \text{ pb}^{-1}$ at RHIC when restricting M to be in the range 5 – 9 GeV. The QCD corrections to the polarized cross section turn out to be largest in the fixed-target regime, whereas the asymmetry receives the largest corrections at higher energies. In most cases the NLO contributions are sizeable and should be included for a meaningful comparison with future data. We note in passing that we found that the dependence of the results on μ_R and μ_F is greatly reduced at NLO.

In Figs. 1 and 2 we also display the statistical errors expected for such measurements of A_{TT} . Here, we try to estimate the influence of detector cuts on the error, which could be rather crucial for making realistic predictions. For instance, if the muon detectors have limited angular coverage, one or both of the muons might escape detection just for geometrical reasons, and the event is lost. In the case of the RHIC detector PHENIX⁴, the endcaps will be able

²The result of [8] is not given in the conventional $\overline{\text{MS}}$ -scheme; however the translation can be easily made.

³In [5] we actually did not saturate the *total* quark distributions, but only their *valence* component at the input scale μ_0 . As was pointed out in [9], this is, strictly speaking, not the statement of the Soffer inequality. A careful numerical check however reveals that none of our results in [5] is altered if one saturates the *full* quark distributions instead of the valence ones.

⁴We only calculate acceptance corrections for PHENIX, since the other major RHIC detector, STAR, cannot detect muons, but only electrons. Electron pair production does not seem as promising as muon pair production, as a very detailed study of the background is required in that case.

to identify muons with $1.2 < |y_{\mu\pm}| < 2.4$; an additional cut on the muon momentum, $|\vec{k}| > 2$ GeV, will probably be necessary to get rid of unwanted background. Central rapidity muon detector arms, which would cover $|y_{\mu\pm}| < 0.35$ (even though for only half of the azimuth), were proposed but will not be realized [10]. Nevertheless, we have also studied the impact that they would have had on the achievable experimental accuracy. In order to calculate the relevant acceptances, the momenta of the outgoing muons must be known. However, they cannot be reconstructed from the kinematic variables M , y , and ϕ introduced above, since M and y refer to the dimuon system and ϕ is only one of the angles describing the direction of one muon. Therefore, one has to consider a more differential cross section, like

$$\frac{d(\delta)\hat{\sigma}^{(0)}}{dMdyd\phi dk_T} = \frac{4\alpha^2}{3SM^3} \frac{(\delta)\zeta(M, k_T, \phi)}{\sqrt{1 - \frac{4k_T^2}{M^2}}} \delta(x_1 - x_1^0)\delta(x_2 - x_2^0), \quad (7)$$

where $\zeta(M, k_T, \phi) = k_T(2 - 4k_T^2/M^2)$, $\delta\zeta(M, k_T, \phi) = 4\cos(2\phi)k_T^3/M^2$, and k_T is the transverse momentum of the muons. The LO acceptance curve for the measurement of, say, the y -dependence of the cross section or the asymmetry A_{TT} , can then be obtained by dividing the results based on Eq. (7), after implementation of appropriate cuts on $y_{\mu\pm}$, by the full LO result, i.e., the one integrated over all k_T and already used in Figs. 1 and 2. Of course one could have also extended the acceptance analysis to NLO, where the muons are no longer back-to-back and the possibility arises that both muons go into the same hemisphere of the detector. However, we believe that a LO estimate for the acceptance is good enough to get a rough quantitative understanding of the influence of limited detector coverage on the statistical error.

Figure 3 shows the acceptances for muon identification in the endcaps only and for the endcaps plus central detector arms. Note that the unpolarized acceptances ε differ from the polarized ones $\delta\varepsilon$ as a result of the different k_T -dependences of the corresponding cross sections (7). The results for $\sqrt{S} = 200$ GeV and 500 GeV turn out to be almost the same, because we used the same lower limit for the dimuon mass M in both cases. According to Fig. 3, the acceptance for the central rapidity region $y \approx 0$, where each endcap or each central arm detects one muon, is considerably smaller than for the large rapidity region, where both muons hit the same endcap. Also, the ratio of “polarized-to-unpolarized acceptance” is smaller than unity in the former case and larger than unity for the latter. This means that the experimentally measured asymmetry will be smaller at $y \approx 0$, but somewhat enhanced at large y as compared to the values given in Fig. 1. We also see that the addition of muon identification in the central arms would yield a much larger acceptance at small and intermediate dimuon rapidities than found for the “endcaps only” scenario.

At the moment, HERA- \vec{N} only has the status of a fairly general proposal for a fixed-target pp spin experiment at HERA [11]. Thus, nothing specific is known yet about appropriate kinematical cuts. In our analysis we try to use reasonable values for the kinematical coverage, keeping in mind that the true detector could look significantly different in case it will ever be built. We use ± 700 mrad for the horizontal and ± 160 mrad for the vertical opening angle, while the beam pipe is assumed to cover ± 10 mrad. Such a detector would have much larger acceptances than PHENIX, as can also be seen in Fig. 3.

Exploiting our LO estimates of the acceptances ε and $\delta\varepsilon$, we are now in a position to calculate the expected statistical errors on the asymmetry. Here we assume that it makes sense to adopt our LO acceptances curve also for the NLO calculation; see our discussion above. The statistical error of the “measured” asymmetry, i.e., *after* correction for acceptance, is then just given by $1/\mathcal{P}^2\sqrt{\mathcal{L}\int\varepsilon d\sigma}$ where \mathcal{P} denotes the degree of polarization of each beam, \mathcal{L} is the integrated luminosity, and the integration goes over the bin under consideration. In order to consistently match the error bars to Figs. 1 and 2, we obviously have to weigh them by the ratio $\frac{\int d\delta\sigma}{\int d\sigma} / \frac{\int \delta\varepsilon d\delta\sigma}{\int \varepsilon d\sigma}$.

The statistical errors show the same features for both RHIC energies. A measurement in the central rapidity region will hardly be possible, even if the central muon detector arms are added. Statistical errors at large rapidities do not depend on the presence of central rapidity muon detection (see Fig. 3), and prospects look slightly better here. The larger rates for $\sqrt{S} = 500$ GeV are compensated by a smaller asymmetry so that, for both $\sqrt{S} = 200$ GeV and $\sqrt{S} = 500$ GeV, the relative statistical error is about 40% at large y . Note that we also include the events with negative rapidity for the calculation of the error bars, since the results are symmetric in y . The situation for HERA- \vec{N} is somewhat better, with relative errors of about 30%, and more possible bins. This is mainly due to the much larger asymmetry in the fixed-target regime. However, for all this we should keep in mind that the asymmetries we show have been obtained assuming saturated δq 's at a low scale. If the saturation were only at, say, the 50% level, then all asymmetries would have to be scaled down by a factor 4, and no measurement would be possible.

Clearly, the restriction in angular acceptance expressed by Fig. 3 will also leave its footprint for the y -integrated, i.e., the total, Drell-Yan cross section. In other words, we have to reinspect our predictions made in [5] for this quantity, to see whether there is any dramatic change concerning the statistical accuracy of a possible measurement of $A_{TT}(M)$.

On the left-hand sides of Figs. 4 and 5 we show the unpolarized and polarized acceptances for the total dimuon cross section for the RHIC energy of $\sqrt{S} = 200$ GeV and the HERA- \vec{N} situation. In the case of RHIC, we distinguish again between the “endcaps only” and the “endcaps plus arms” options. The general trend is that the acceptances are rather low for RHIC (PHENIX) and decrease with increasing M after reaching a peak at a quite low M -value. Under our assumed conditions for HERA- \vec{N} , the acceptance turns out to be much higher and fairly independent of M . On the right-hand sides of Figs. 4 and 5 we redisplay our findings for $A_{TT}(M)$ of Figs. 3 and 4 of Ref. [5], but now with the more realistic error bars based on our considerations concerning the acceptance. One finds that at not too large M , a measurement of a non-vanishing asymmetry for the total Drell-Yan cross section still looks possible also for RHIC, provided the “true” transversity densities are anywhere near the ones we have modeled. Measurements at large M appear hopeless. The situation for $\sqrt{S} = 500$ GeV at RHIC is qualitatively very similar and hence not shown. Again, as in the case of $A_{TT}(y)$, HERA- \vec{N} looks in a somewhat better shape.

In conclusion, we have studied the “maximally possible” A_{TT} , resulting from saturation of Soffer’s inequality at a low hadronic scale. It turns out that the limited muon acceptance for the RHIC experiments threatens to make a measurement of transversity elusive. In particular, it will be difficult, if not impossible, to measure the rapidity dependence of A_{TT} , which in principle would be expected to be sensitive to the *shape* of δq . At best, one data point at large y can be obtained, but with a large relative error. The limitation in the muon acceptance also affects the y -integrated cross section, so that the resulting $A_{TT}(M)$ will also receive a substantial relative statistical error. An upgrade of the PHENIX detector towards muon identification also in the central arms would not improve the situation significantly. Lower energies, in combination with better muon acceptance, seem more favorable.

ACKNOWLEDGMENTS

We thank G. Bunce and N. Saito for useful information concerning the RHIC detector acceptances. Furthermore, we are indebted to W.-D. Nowak for very valuable discussions about HERA- \vec{N} . W.V. is grateful to D. de Florian for useful discussions. O.M. and A.S. acknowledge financial support from the BMBF and the “Deutsche Forschungsgemeinschaft”. This work was supported in part by the EU Fourth Framework Programme “Training and Mobility of Researchers”, Network “Quantum Chromodynamics and the Deep Structure of Elementary Particles”, contract FMRX-CT98-0194 (DG 12 - MIHT).

-
- [1] RHIC Spin Collab., D. Hill et al., Letter of intent RHIC-SPIN-LOI-1991, updated 1993; G. Bunce et al., Particle World **3**, 1 (1992); PHENIX/Spin Collaboration, K. Imai et al., BNL-PROPOSAL-R5-ADD (1994).
 - [2] J.P. Ralston and D.E. Soper, Nucl. Phys. **B152**, 109 (1979); R.L. Jaffe and X. Ji, Phys. Rev. Lett. **67**, 552 (1991); Nucl. Phys. **B375**, 527 (1992); X. Artru and M. Mekhfi, Z. Phys. **C45**, 669 (1990).
 - [3] J. Soffer, Phys. Rev. Lett. **74**, 1292 (1995).
 - [4] W. Vogelsang, Phys. Rev. **D57**, 1886 (1998).
 - [5] O. Martin, A. Schäfer, M. Stratmann, and W. Vogelsang, Phys. Rev. **D57**, 3084 (1998).
 - [6] J. Soffer and O. Teryaev, Phys. Lett. **B420**, 375 (1998).
 - [7] W. Vogelsang and A. Weber, Phys. Rev. **D48**, 2073 (1993).
 - [8] P. Sutton, A.D. Martin, R.G. Roberts, and W.J. Stirling, Phys. Rev. **D45**, 2349 (1992).
 - [9] Y. Kanazawa, Y. Koike, and N. Nishiyama, Phys. Lett. **B430**, 195 (1998).
 - [10] N. Saito, private communication.
 - [11] V.A. Korotkov and W.-D. Nowak, Nucl. Phys. **A622**, 78c (1997).

FIGURE CAPTIONS

Fig. 1 “Maximal” polarized cross section and asymmetry as functions of dimuon rapidity y for RHIC at $\sqrt{S} = 500$ GeV. The error bars have been calculated for $\mathcal{L} = 800 \text{ pb}^{-1}$, 70% polarization of both beams, and include acceptance corrections (see text). The point at low rapidity can only be obtained if PHENIX is endowed with central muon detector arms.

Fig. 2 Same as Fig. 1, but for HERA- \vec{N} with $E_{\text{beam}} = 820$ GeV and $\mathcal{L} = 240$ pb $^{-1}$.

Fig. 3 Acceptance curves for the detection of dimuons with the PHENIX and HERA- \vec{N} detectors, as functions of the dimuon rapidity y . The PHENIX acceptances for $\sqrt{S} = 500$ GeV and $M = 5$ – 20 GeV differ only very slightly from the results shown here for the case $\sqrt{S} = 200$ GeV.

Fig. 4 Dependence of the acceptances and the NLO asymmetry A_{TT} on the dimuon invariant mass, integrated over rapidity, for $\sqrt{S} = 200$ GeV at RHIC. The error bars on the right-hand side include the acceptance corrections and are based on $\mathcal{L} = 320$ pb $^{-1}$ and $\mathcal{P} = 0.7$. The outer error bars correspond to the “endcaps only” option, while the inner ones have been obtained assuming additional central detector arms.

Fig. 5 Same as Fig. 4, but for $\sqrt{S} = 39.2$ GeV, corresponding to HERA- \vec{N} .

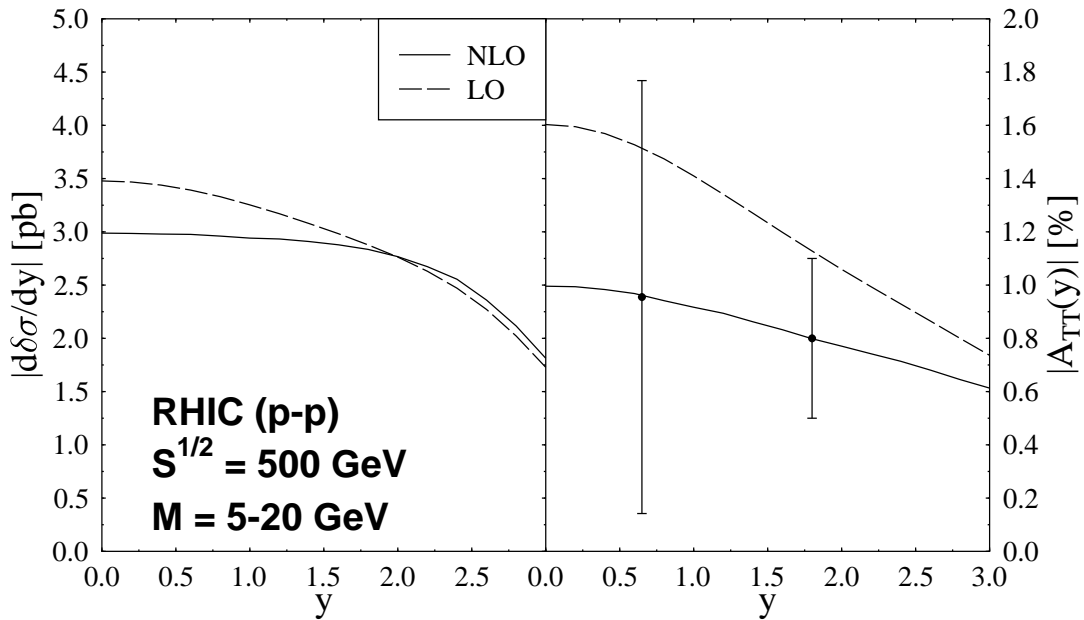


Fig. 1

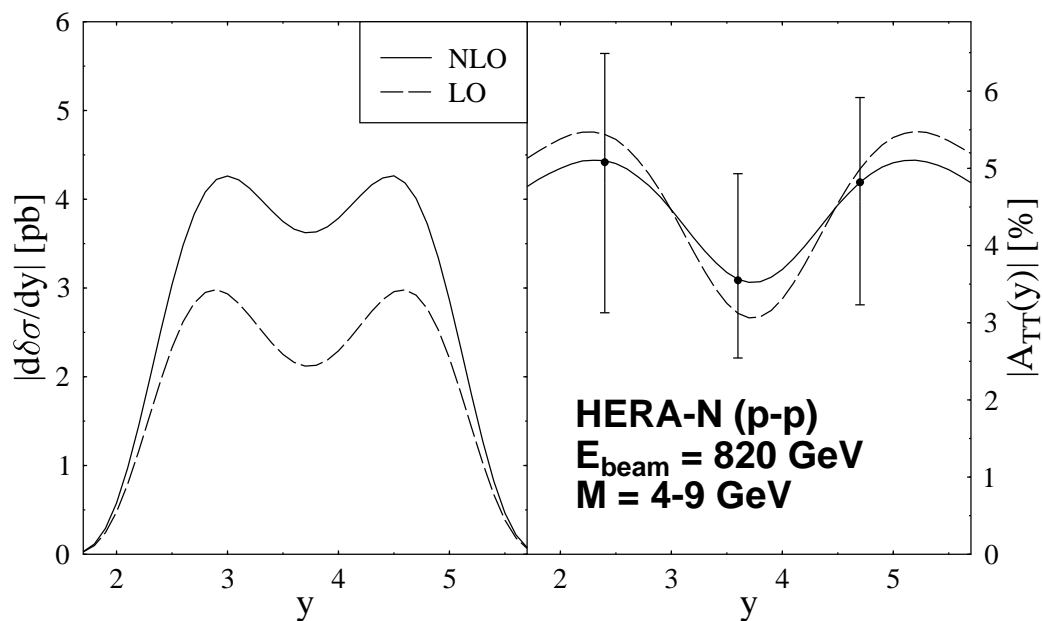


Fig. 2

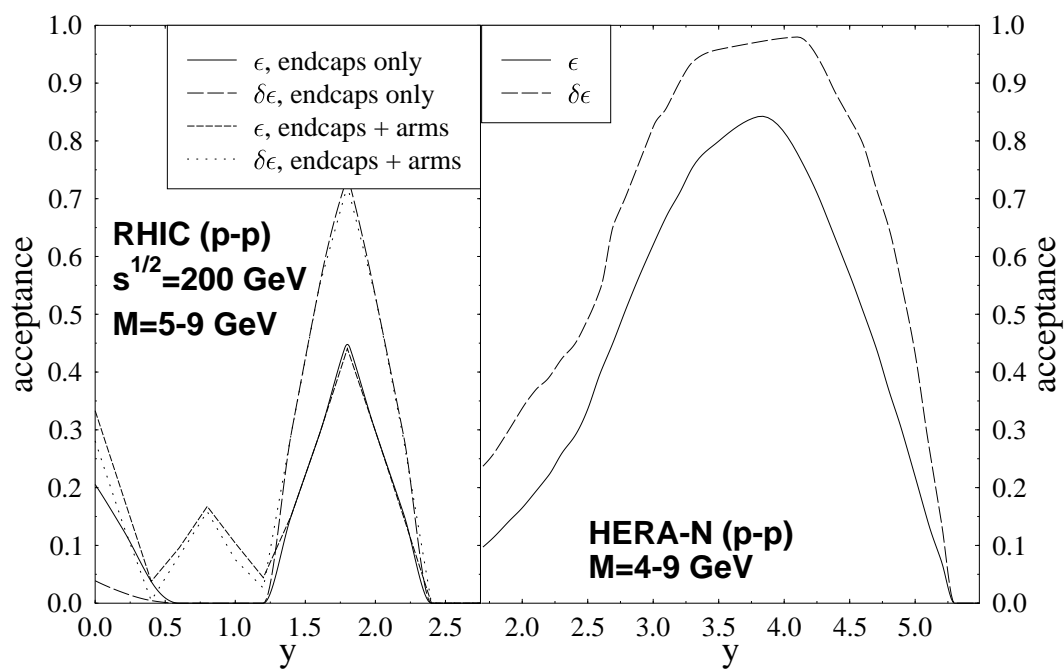


Fig. 3

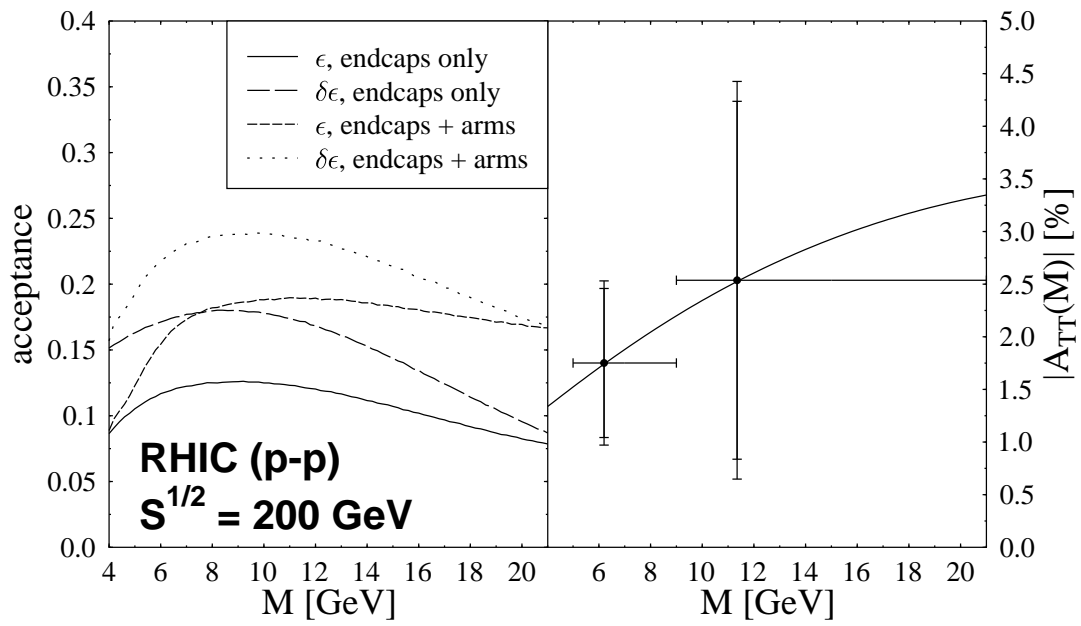


Fig. 4

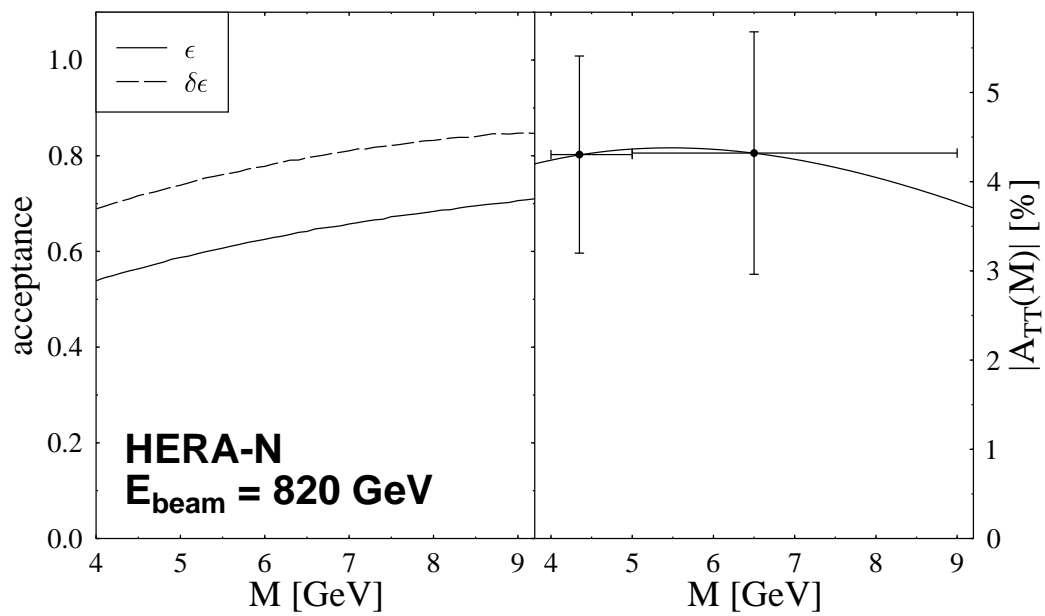


Fig. 5